

# In Vitro Morphophysiological Responses of *Alternanthera Tenella Colla* (Amaranthaceae) to Stress Induced by Cadmium and the Attenuating Action of Silicon

**Franciele Pereira Rossini**

Federal University of Espirito Santo: Universidade Federal do Espirito Santo

**João Paulo Rodrigues Martins** (✉ [jprmartinss@yahoo.com.br](mailto:jprmartinss@yahoo.com.br))

Polish Academy of Sciences Institute of Dendrology Kornik: Polska Akademia Nauk Instytut Dendrologii w Korniku <https://orcid.org/0000-0003-0554-6793>

**Samuel Werner Moreira**

Federal University of Espirito Santo: Universidade Federal do Espirito Santo

**Lorenzo Toscano Conde**

Federal University of Espirito Santo: Universidade Federal do Espirito Santo

**Evens Clairvil**

Federal University of Espirito Santo: Universidade Federal do Espirito Santo

**Priscila da Conceição de Souza Braga**

Federal University of Espirito Santo: Universidade Federal do Espirito Santo

**Antelmo Falqueto**

Federal University of Espirito Santo: Universidade Federal do Espirito Santo

**Andreia Barcelos Passos Lima Gontijo**

Federal University of Espirito Santo: Universidade Federal do Espirito Santo

---

## Research Article

**Keywords:** plant anatomy, plant physiology, phytoremediation, trace element

**Posted Date:** January 12th, 2022

**DOI:** <https://doi.org/10.21203/rs.3.rs-1236364/v1>

**License:**   This work is licensed under a Creative Commons Attribution 4.0 International License.

[Read Full License](#)

---

**Version of Record:** A version of this preprint was published at Plant Cell, Tissue and Organ Culture (PCTOC) on March 8th, 2022. See the published version at <https://doi.org/10.1007/s11240-022-02263-y>.

# Abstract

Despite having the ability to bioaccumulate trace elements such as cadmium (Cd), many species also present morphophysiological disorders that can hamper their use as phytoremediation plants. Since it can lead to alterations in biomass accumulation. The employment of elements that mitigate stress, such as silicon (Si), can diminish the deleterious effects caused by trace elements. The objective of this study was to analyze the anatomical and physiological modulations induced by the synergy between Cd and Si in *Alternanthera tenella* plants, as well as to elucidate whether Si can mitigate the harmful effects caused by Cd under in vitro conditions. Nodal segments were cultured in media containing a concentration gradient of Cd (0, 50, 100, or 200  $\mu\text{M}$ ) combined with two levels of Si (0 or 40  $\mu\text{M}$ ) for a total of eight treatments. After 34 days, the plants' anatomy, physiology, and tolerance index were analyzed. The plants presented anatomical adjustments (such as lower stomatal index and number of vessel elements), suggesting lower translocation of Cd to the aerial part. When cultured with 200  $\mu\text{M}$  Cd, the plants presented the lowest Chl *a/b* ratio. In the presence of Si, the decline of this ratio was smaller. Plants exposed to Cd concentrations of 50  $\mu\text{M}$  without Si presented a significant decrease in the performance of the photosynthetic apparatus and tolerance index. The presence of Si in the medium reduced the damages caused by cadmium to the plants' physiology, resulting in greater growth and higher tolerance to this element.

# Introduction

There is a growing concern about pollution of ecosystems with wastes from anthropogenic actions, especially residues that contain high levels of trace elements such as cadmium (Cd), copper (Cu), chrome (Cr), lead (Pb), zinc (Zn), aluminum (Al), manganese (Mn) and mercury (Hg). These elements, even in small quantities, are highly bioaccumulative at all levels of the trophic chain (Suman et al. 2018; Hu et al. 2020).

Among these metals, Cd stands out for its easy uptake and high mobility and accumulation in the structures of plants, where it can cause an imbalance in the system for uptake of water and nutrients by competing for bonding sites, as well as damaging the photosynthetic apparatus and modifying the leaf morphology and anatomy (Rodrigues et al. 2017; Dobrikova et al. 2021).

Various methods have been employed to minimize the effects of Cd contamination of ecosystems, ranging from the use of physical-chemical methods to the use of living organisms, such as plants, bacteria, and fungi that can extract and store high concentrations of this metal in their structure (Liu et al. 2018; Roychowdhury et al. 2018; Haider et al. 2021). Besides this, studies have shown that the cultivation of plants with the presence of stress-mitigating elements such as selenium (Se) and silicon (Si) is promising to diminish the deleterious effects of trace elements on the plants' systems (Ding et al. 2017; Martins et al. 2020a; Haider et al. 2021; Huang et al. 2021). However, more comprehensive studies are necessary to understand better the relationship among plants, heavy metals, and stress-mitigating

elements to ascertain whether this mitigation is really feasible as part of a strategy for the recovery of ecosystems.

Among the stress-mitigating elements, Si stands out for being the second most abundant element in the Earth's crust and having a high affinity for alkaline and alkaline-earth metals (Menegale et al. 2015). Plants' need for Si has been discussed by various researchers (Menegale et al. 2015; Klotzbücher et al. 2018; Bari et al. 2020; Chung et al. 2020). The results of these studies have shown the participation of Si in the regulation of morphological, physiological, and genetic responses of various plants, aiming at the reduction of abiotic and biotic stress. Among these are an increased uptake and assimilation of mineral nutrients; modulation of the antioxidant system; increases of the photosynthetic rate, stomatal conductance, and concentration of CO<sub>2</sub>; and reduction of the transpiration rate (Etesami and Jeong 2018; Malhotra and Kapoor 2019).

Several studies have reported the effects of Si to increase the tolerance and/or reduce the impact of toxicity caused by trace elements in many plant species (Gu et al. 2011; Pereira et al. 2018; Vaculík et al. 2020; Ur-Rahman et al. 2021). These effects include reduction of the uptake of these elements by the plant, alteration of the content of photosynthetic pigments, compartmentation in metabolically inactive parts, co-precipitation of metals with Si, chelation, and modification of the genetic expression in some species (Adrees et al. 2015; Emamverdian et al. 2018; Etesami and Jeong 2018; Bhat et al. 2019; Cai et al. 2020). Therefore, a better understanding of how Si can mitigate stress in plants with phytoremediation potential is important to optimize their performance in this respect.

The joint application of techniques to observe plant anatomy, quantify the content of photosynthetic pigments, and analyze the chlorophyll *a* fluorescence transients on in vitro culture conditions allows comparing the alterations promoted by the presence of a trace element and/or supplementation with other elements precisely, without the interference of external factors (Martins et al. 2020b; Guo et al. 2020), besides elucidating the effects caused in photosystem II and I (PSII and PSI), among other morphophysiological responses of plants (Pereira et al. 2017; Guo et al. 2020; Martins et al. 2021)

Previous studies have already reported the potential of *Alternanthera tenella* Colla (Amaranthaceae) for bioaccumulation of Cd and Cu (Rodrigues et al. 2017; Martins et al. 2020b). This species is herbaceous, with rapid growth and high biomass production. However, Rodrigues et al. (2017) found that when cultured in vitro, the growth of plants of this species declined when submitted to high Cd concentrations, which can negatively influence its employment for phytoremediation. Thus, the objective of this work was to analyze the anatomical and physiological modulations induced by the synergy of Cd and Si in *A. tenella* plants, as well as to elucidate whether Si can mitigate the deleterious effects caused by Cd.

## Material And Methods

### Exposure to cadmium and silicon during in vitro culture

*A. tenella* plants were previously established and multiplied in vitro according to the method proposed by Rodrigues *et al.* (2017). Plants with similar morphology (after the multiplication phase without plant growth regulators) were used as the source of explants (nodal segments with an approximate length of  $2 \pm 0.5$  cm). The segments were transferred to 500 mL flasks containing 30 mL MS medium (Murashige and Skoog 1962) supplemented with  $20 \text{ g L}^{-1}$  sucrose (Dinâmica<sup>®</sup>, Brazil) and  $6 \text{ g L}^{-1}$  agar (Dinâmica<sup>®</sup>, Brazil). Cadmium (Cd) was added to the culture medium in a concentration gradient of 0, 50, 100 or 200  $\mu\text{M}$ , in the form of  $\text{Cd}(\text{NO}_3)_2 \cdot 4\text{H}_2\text{O}$ , combined with two levels of silicon (0 or  $40 \mu\text{M Si} - \text{CaSiO}_3$ ), for a total of 8 treatments. The Si levels were determined through a previous experiment in which the morphophysiological responses of the plants were analyzed in function of Si levels. The media's pH was adjusted to 5.8 before autoclaving at  $120 \text{ }^\circ\text{C}$  for 20 minutes. All the procedures for inoculation of the plants were performed in aseptic conditions in a laminar flow cabinet. The plants were subsequently maintained in a growth room at  $26 \pm 2 \text{ }^\circ\text{C}$  with 16:8 hour photoperiod under Slim LED lamps (Blumenau<sup>®</sup> 36W/6500K), supplying  $70 \mu\text{mol m}^{-2} \text{ s}^{-1}$  of photosynthetically active radiation, for a period of 34 days.

### **Leaf anatomy**

For anatomical characterization, after cultivation for 34 days, four plants from each treatment were collected at random and fixed in FAA (formaldehyde, acetic acid, and 50% ethanol at 0.5/0.5/9.0 v/v) for 72 h, after which the material was preserved in 50% (v/v) ethanol until analysis (Johansen, 1940). Transversal and paradermal sections were obtained from the first pair of fully expanded leaves. The slides were prepared according to Martins *et al.* (2020b) and were photographed with a digital camera (Leica ICC50 HD<sup>®</sup>, Wetzlar, Germany) coupled to a light microscope (Bioval, L-2000A-Flur<sup>®</sup>). The anatomical measurements ( $n = 4$ ) were carried out with the Imagetool<sup>®</sup> software, calibrated with a microscopic ruler. The anatomical traits analyzed were: the thickness of the palisade ( $\mu\text{m}$ ) and spongy parenchyma ( $\mu\text{m}$ ), stomatal density ( $0.1 \text{ mm}^{-2}$ ), stomatal index (%), epidermal cell density ( $0.1 \text{ mm}^{-2}$ ), and the number of vessel elements.

### **Quantification of the content of photosynthetic pigments**

The quantification of the contents of chlorophyll *a* and *b* (Chl *a* and Chl *b*), and total chlorophyll (Chl *total*) was performed at the end of the experiment, according to the method proposed by Arnon (1949). For this purpose,  $0.02 \pm 0.005$  g of fresh weight from the second pair of fully expanded leaves was weighed, and the pigments were extracted with 5 mL of 80% (v/v) acetone for 72 hours in the dark at a constant temperature of  $4 \text{ }^\circ\text{C}$ . The absorbance levels were read with a Genesys<sup>™</sup> 10S UV-Vis spectrophotometer (Thermo Fisher Scientific, West Palm Beach, FL, USA), with wavelengths of  $\lambda = 645$  and 665 nanometers (nm) for Chl *b* and Chl *a*, respectively. The calculations were performed as described by Wellburn (1994), and the results ( $n = 8$ ) are expressed in micrograms of pigment per gram of fresh weight ( $\mu\text{g g}^{-1}$  FW).

### **Analysis of chlorophyll *a* fluorescence transients**

The chlorophyll *a* fluorescence transients (OJIP) were determined with a portable fluorometer (Handy PEA<sup>®</sup>/ Hansatech Instruments Ltd., King's Lynn, Norfolk, UK). For this purpose, the second pair of fully expanded leaves (from the tips and not detached) of 18 different plants ( $n = 18$ ) from each treatment were previously adapted to the dark for 30 min with leaf clips (Hansatech<sup>®</sup>). The fluorescence emission was induced in a circular area with a diameter of 4 mm by exposure of the sample to a saturating red-light pulse (peak 650 nm), and the intensity of  $3,000 \mu\text{mol m}^{-2} \text{s}^{-1}$  was recorded and used to calculate the parameters of the JIP test and the relative variable fluorescence between the steps O and P ( $V_{OP}$ ), steps O and K ( $V_{OK}$ ), and steps O and J ( $V_{OJ}$ ) (Strasser et al. 2004; Stirbet and Govindjee 2011; Guo et al. 2020) using the BioLyzer software (Bioenergetics Laboratory, University of Geneva, Switzerland). The  $W_L$  and  $W_K$  were calculated according to Zhang et al. (2018).

### **Growth traits and tolerance index**

To evaluate the in vitro growth, 25 plants from each treatment were collected at random, divided into 5 replicates ( $n = 5$ ), and weighed on an analytical balance (ATY 224, Shimadzu). The aerial parts and roots were weighed separately to determine grams per plant ( $\text{g plant}^{-1}$ ). After determining the fresh weight, the samples were dried in a forced-air oven (AC-035/480, Acblabor) for 72 hours at 70 °C, and the aerial parts and roots were weighed again.

The tolerance index (TI) was calculated as proposed by Wilkins (1957), with modifications, by dividing the total dry weight of the plant from each treatment by the total dry weight of the control plant (0  $\mu\text{M}$  Si + 0  $\mu\text{M}$  Cd). The values obtained ( $n = 5$ ) were multiplied by 100 to express the TI in percentage (%).

### **Statistical analysis**

The experimental design was completely randomized in a 2 x 4 factorial scheme (presence or absence of Si x Cd concentration of 0, 50, 100, or 200  $\mu\text{M}$ ). The data were submitted to analysis of variance (ANOVA), and the means were compared by the Tukey test at 5% significance using the *ExpDes* package of R (Ferreira et al. 2018).

## **Results**

### **Characterization of leaf anatomy**

Alterations of the leaf anatomy of the *A. tenella* plants were observed in the function of the treatments. The stomatal density was influenced by both variation factors (Cd and Si), but the influence was independent. The number of stomata per area declined with increasing concentrations of Cd. Between the two Si levels, the plants cultured with 40  $\mu\text{M}$  Si presented greater stomatal density than those cultivated without this element (Figs. 1 and 2A).

There was a significant interaction between Cd and Si for stomatal index and epidermal cell density. In the absence of Si, the stomatal index declined with rising Cd concentration. When Si was added to the

culture medium, both characteristics presented similar values irrespective of the Cd concentrations. The plants exposed to 200  $\mu\text{M}$  Cd but without Si had greater epidermal cell density and the lowest stomatal index among the treatments (Fig. 1 and Table 1).

In the transversal sections, the parenchyma thickness was also influenced by the Si and Cd. The supplementation of Si, as well as Cd, induced a thinner palisade parenchyma, especially when the plants were exposed to 100 and 200  $\mu\text{M}$  Cd. In the spongy parenchyma, the addition of 50 and 100  $\mu\text{M}$  of Cd to the medium caused a reduction of its thickness, regardless of the level of Si. In turn, the results of the treatments with 0 and 200  $\mu\text{M}$  of Cd were statistically similar between each other regarding these two conditions (Fig. 1 and Table 1).

The number of vessel elements was only altered by the concentrations of Cd. The exposure to this trace element induced leaves with fewer vessel elements (Figs. 1 and 2B).

### **Photosynthetic pigment content**

The variation factors (Si and Cd) influenced the content of photosynthetic pigments. The plants cultivated with Si had larger values for all the pigment contents when exposed to Cd concentrations up to 50  $\mu\text{M}$ . While at higher Cd concentrations, the plants presented a steep decline of the contents of all the pigments, irrespective of the presence or absence of Si in the culture medium (Figs. 3A-B, 3D). Also, in the absence of Si, the plants exposed to 200  $\mu\text{M}$  Cd had the smallest Chl *a/b* ratios among the treatments (Fig. 3C).

### **Chlorophyll *a* fluorescence transients**

Independent of the treatment, the plants remained photosynthetically active. The relative fluorescence values revealed large increases as of step L in the plants cultured with 200  $\mu\text{M}$  Cd, regardless of the level of Si (Figs. 4A-B). These responses were confirmed by the significant increases in the values of  $V_L$ ,  $V_K$ ,  $V_J$ , and  $V_I$ . The values of  $V_J$  and  $V_I$  presented an interaction between the variation factors. Exposure to Cd led to significant increases of  $V_J$  and  $V_I$ , mainly at the highest concentrations of this trace element. When comparing the Si levels at each Cd concentration, the plants cultivated with 0 and 100 of Cd presented lower values of  $V_I$  in the presence of Si than those grown without Si (Figs. 4A-F).

Analysis of the differences between steps O and K (L-band) revealed the formation of a positive L-band in the plants exposed to 200  $\mu\text{M}$  Cd and under Si absence. In the presence of Si, the amplitudes of the curves were very slight, and there was no clear L-band formation. In the plants cultivated with 200  $\mu\text{M}$  Cd, the formation of positive K-bands (between steps O and J) was verified, irrespective of the Si concentration (Figs. 5A-D). These responses were confirmed by the increased values of  $W_L$  and  $W_K$  in these treatments (Figs. 5E-F).

For all the parameters of the JIP test analyzed, there was an interaction between the factors studied. Cadmium, mainly at the highest concentration, induced a reduction of the values of  $F_V/F_0$ ,  $\phi P_0$ ,  $\phi E_0$ ,  $\delta R_0$ ,

RC/ABS,  $PI_{(ABS)}$ , and  $PI_{(Total)}$ . In these same conditions, the values of  $\phi D_0$  increased. Comparison of the values of these parameters in each Si level, plants cultured under Si absence had more pronounced reductions of  $F_V/F_0$ ,  $\phi P_0$ ,  $\phi E_0$ ,  $\delta R_0$ , RC/ABS,  $PI_{(ABS)}$ , and  $PI_{(Total)}$  than those cultivated with 40  $\mu\text{M}$  Si. The increases of the values of  $\phi D_0$  were also more substantial in the plants exposed to Cd without co-exposure to Si (Fig. 6).

Significant differences between the treatments were also observed in the specific flows of energy for each PSII reaction center. Plants cultivated with 200  $\mu\text{M}$  Cd had higher ABS/RC and  $DI_0/RC$  values, and these increases were greater in the absence of Si (Fig. 7). Among the treatments with Cd and the absence of Si, the values of  $TR_0/RC$  were greater in the plants exposed to 200  $\mu\text{M}$  Cd. In contrast, when Si was added to the culture medium, there was a decrease of  $TR_0/RC$  in the plants co-exposed to Cd. Further regarding the  $TR_0/RC$ , under Cd absence, its values were higher in the plants cultured with 40  $\mu\text{M}$  Si than in those grown without Si. The opposite effect was observed in the treatments with 200  $\mu\text{M}$  Cd since the plants without Si had higher values of  $TR_0/RC$  than those grown with 40  $\mu\text{M}$  Si (Fig. 7). In general, the plants cultivated without Si had lower values of  $ET_0/RC$  than those grown with 40  $\mu\text{M}$  Si at each Cd level (Fig. 7).

### **Growth traits and tolerance index**

All the growth traits presented significant interactions between the variation factors. Furthermore, from a morphological standpoint, the plants exposed to high Cd concentrations had reduced stem length and leaf size, principally at the highest Cd concentration (data not shown). Irrespective of the addition of Si in the medium, there was a gradual reduction of plants' fresh and dry weights in the function of rising Cd concentration. However, this weight reduction was less pronounced in the treatments with Si supplementation (Table 2). The exposure to high Cd concentrations reduced the tolerance index (TI) values, but this decrease was smaller for the plants cultivated with the presence of Si (Table 2).

## **Discussion**

In this study, we investigated the interaction between Si and Cd during the in vitro culture of *A. tenella*. The addition of Si to the culture medium resulted in plants that were more tolerant of the stress caused by Cd.

Alterations in the leaf anatomy play a fundamental role in plants' adjustment to environmental conditions. In this study, the first stress-regulation mechanisms were related to the investment in the number of stomata (stomatal density and stomatal index) in the function of Cd concentrations. These adjustments in anatomy were reflected in a decrease of the transpiration rate and mass flow, diminishing the uptake and translocation of mineral elements present in the soil or culture medium to the aerial part (Pereira et al. 2017; Martins et al. 2020; Pires-Lira et al. 2020). These alterations were in line with the number of vessel elements (xylem). A smaller number of vessels tends to reduce the translocation of water and nutrients, as well as of Cd, to the aerial part of the *A. tenella* plants. This observation is in

accordance with the Hagen-Poiseuille law, which indicates that a reduction in the vessel elements' number and/or diameter has a negative exponential effect on the water conductivity (Scholz et al. 2013). Therefore, these combined alterations of the stomatal architecture and vessel elements might have been preponderant in controlling the translocation of Cd in the *A. tenella* plants.

The smaller flow of nutrients and water from the culture medium influenced the morphogenesis of the parenchyma tissues. The palisade parenchyma thickness declined, mainly in the plants grown with 100 and 200  $\mu\text{M}$  of Cd. The reduced thickness of this tissue can be related to the smaller translocation of water, which interferes with cell expansion (Silva-Cunha et al. 2021). This process is fundamental for the growth of cell size and thus of the tissue as a whole. Likewise, the exposure to Cd led to thinner spongy parenchyma, correlated with the reduced size of the cells. Reducing this size is a mechanism to maintain functionality under stressful conditions because smaller cells tend to have a greater ability to maintain their turgor when exposed to water shortage than larger cells (Corso et al. 2020). Nevertheless, the plants cultivated with 200  $\mu\text{M}$  Cd, regardless of the presence of Si, had thicker but statistically similar spongy parenchyma than the plants cultivated without Cd. This increase in the spongy parenchyma thickness of the plants exposed to 200  $\mu\text{M}$  Cd was correlated with an increase in the intercellular spaces but not with the size of the cells. It makes sense because the intercellular spaces of the spongy parenchyma have the function of maximizing the surface area available for light capture and gas exchange for photosynthesis (Zhang et al. 2021). Besides this, the formation of larger intercellular spaces in spongy parenchyma can optimize the accumulation of  $\text{CO}_2$  and the accessibility of carboxylation sites on the chloroplasts inside the leaf cells (Acosta-Motos et al. 2015; Paradiso et al. 2017), in turn requiring less frequent stomatal opening for gas exchange. This morphological response of the spongy parenchyma is often related to water deficit (Acosta-Motos et al. 2015; Rouphael et al. 2017; Mott and Peak 2018). In this study, the *A. tenella* plants cultivated with 200  $\mu\text{M}$  Cd presented an accentuated reduction in leaf size (leaf area) besides thicker spongy parenchyma. This suggests a compensatory mechanism (tradeoff) to maximize the accumulation of  $\text{CO}_2$  and minimize the evapotranspiration, preventing an increase in the mass flow and translocation of Cd.

One of the ways to determine physiological alterations and damages to the photosynthetic apparatus is by quantifying the contents of photosynthetic pigments in the leaves since plants under stress tend to have lower contents and modifications of their proportions to balance the levels and/or reduce the damages to the photosystem (Janečková et al. 2019). In the present study, we observed reductions in the contents of Chl *a*, Chl *b*, Car, and Chl<sub>Total</sub> with rising concentrations of Cd in the culture medium, independently of the presence or absence of Si. Cd can cause modifications in the structure of the photosynthetic pigments due to competition for the binding sites of  $\text{Mg}^{2+}$  in the pheophytin ring and/or inhibition of the synthesis of the enzyme 5-aminolevulinic acid, which plays an important role in the biosynthesis of chlorophylls (Grajek et al. 2020); besides overloading of the antioxidant system, causing misshapen chloroplasts, dilation of thylakoid membranes and instability of chlorophyll (Pereira et al. 2017; Rodrigues et al. 2017). However, in the presence of Si, this decrease was less severe. That response might have been associated with the improvement of the antioxidant system, and therefore lesser

oxidative damages of the structure and function of the thylakoid membranes (Yanhui et al. 2020). That hypothesis is corroborated by the values of  $W_L$  obtained.

The Chl *a/b* ratio is a good indicator of how plants respond to the influence of metals on their photosynthetic apparatus (Ranjbarfordoei et al. 2006; Martins et al. 2020a, b; Houry et al. 2020). In this study, we observed a coordinated reduction of Chl *a* and *b*, but no significant change in the ratio, particularly in the treatments with 50 and 100  $\mu\text{M}$  of Cd, indicating the efficacy of the plants' metabolism in minimizing the harmful effect of the excess of this metal. In contrast, the reduction of Chl *a/b* ratio in the treatment with 200  $\mu\text{M}$  Cd indicated an imbalance between the contents of Chl *a* and Chl *b*, besides a high degradation rate of Chl *a*. In the presence of Si, the Chl *a/b* ratio of plants exposed to 200  $\mu\text{M}$  Cd did not decline as much as in the plant cultivated with the same concentration of Cd but without Si. This response denotes lesser degradation of Chl *a*, indicating less damage to the active reaction centers (RCs) and hence in the performance of photosystem II (PSII) (Martins et al. 2021).

Alterations in the performance of the photosynthetic apparatus also demonstrated the effects of co-exposure to Si and Cd. A point-by-point analysis of the OJIP curve revealed the influence of this co-exposure and the response in the apparatus. At points  $V_L$  and  $V_K$ , we observed an increase in the plants grown with 200  $\mu\text{M}$  Cd, irrespective of the presence of Si. This alteration at the highest Cd concentration indicated less energy connectivity of the PSII units and less efficiency of the oxygen-evolving complex (OEC) (Brestic et al. 2012; Begovic et al. 2020; Martins et al. 2020b). According to Zhang et al. (2018), an increased value of  $V_K$  can be considered a specific marker of damage to the activity of the OEC from the electron donor side of PSII. In turn, alterations of the values of  $V_J$  and  $V_I$  indicate the functioning of electron transport between the quinones ( $Q_A$  and  $Q_B$ ) on the receptor side of PSII and changes in the efficiency/probability of movement of electrons between the photosystems, respectively (Santos et al. 2020; Martins et al. 2021). In this study, we observed that the presence of Si was associated with better electron transfer between the quinones and between PSII and PSI.

Another indicator to identify physiological disorders before visual manifestations of damage is the appearance of L- and K-bands. Positive L-bands indicate disturbances in the thylakoid membranes, reducing the connectivity between the CRs and PSII and causing less energy clustering among the photosystem units (Strasser et al. 2004). In other words, the behavior was denoted by an inverse function, in which a higher positive amplitude of band-L is associated with lesser connectivity. A positive band-K is closely related to an inactivation of the OEC (Xiang et al. 2013). We observed that the connectivity between CRs was maintained in the treatment with the highest concentration of Cd and the addition of Si. This maintenance may be attributed to the improvement of the antioxidant system, causing the values of  $W_L$  to decline. According to Zhang et al. (2018), lower values of this parameter denote better functional and structural integrity of the thylakoid membranes. In counterpart, we observed an increase of the amplitude of band-K and the values of  $W_K$  in the treatments with 200  $\mu\text{M}$  Cd regardless of the presence of Si. This elevation might have been due to water restriction caused by the reduction of water connectivity (a characteristic determined by the stomatal and vessel elements), in turn causing an imbalance between

the transfer of electrons from the OEC to P680<sup>+</sup> and the electron acceptors of Q<sub>A</sub>, along with possible partial inhibition of the water-splitting system.

The association among  $F_V/F_0$ ,  $\phi P_0$ , and  $\phi E_0$  allows analyzing the status of the electron transport system and the efficiency of the trapping, conversion, and transport of energy between the two photosystems (Strasser et al. 2004; Guo et al. 2020). In this respect, the presence of Cd caused a reduction of the values of  $\phi P_0$ ,  $F_V/F_0$ , and  $\phi E_0$  in the treatment with 200  $\mu\text{M}$  Cd, resulting in lower photosynthetic apparatus efficiency. In contrast, when the plants were co-exposed to Cd and Si, the decrease in the values of those parameters were not as great (in relation to the control treatment), serving as an indicator of maintenance of the system for trapping, conversion, and transport of energy. This could have caused lesser dissipation of the energy ( $\phi D_0$ ).

The exposure to Cd also generated an increase in the values of  $\text{ABS}/\text{RC}$ ,  $\text{TR}_0/\text{RC}$ , and  $\text{DI}_0/\text{RC}$ , indicating the susceptibility of the plants to photoinhibition caused by the down-regulation of the mechanism for dissipation of the energy absorbed by the reaction center (RC) (Franić et al. 2018). However, the presence of Si generated an adjustment that ameliorated the damages caused by the Cd. This improvement triggered an increase of  $\text{ET}_0/\text{RC}$  and reduced energy loss by dissipation. At the highest Cd concentration, the Si also caused a less pronounced reduction of  $\text{RC}/\text{ABS}$ , corroborating the results found for the  $\text{Chl } a/b$  ratio.

The performance indices  $\text{PI}_{(\text{ABS})}$  and  $\text{PI}_{(\text{Total})}$  indicate how the stress factors affect the performance and integrity of the photosynthetic apparatus of plants (Kalaji et al. 2016). In particular, because  $\text{PI}_{(\text{ABS})}$  represents the combination of three factors (total number of active reaction centers for absorption of light; trapping of excitation energy; and conversion of that energy into the transport of electrons in PSII), and this parameter is sensitive to the stress caused by the metal (Martins et al. 2020; Guo et al. 2020). Therefore, the presence of Si reduced the damage to the system for trapping of excitation energy, resulting in a better performance of PSII, mainly at the highest Cd concentration. The Si also acted to reduce the photodamage beyond the intersystem, mainly at the highest Cd concentration, confirmed by the increased values of  $\text{PI}_{(\text{Total})}$ . According to Guo et al. (2020), the increase of this parameter when plants are facing high stress is an indicator of improved ability to achieve photochemical reactions, *i.e.*, their efficiency in using the energy absorbed by the antennas for conversion into energy in the form of ATP and NADPH, resulting in better physiological conditions for development and survival.

In summary, the presence of Si in the culture medium caused a reduction of the damages caused by Cd in the physiology of the plants, resulting in greater *in vitro* growth. In plants cultured with 40  $\mu\text{M}$  Si, there was a greater biomass accumulation, mainly at the Cd concentrations of 100 and 200  $\mu\text{M}$ , compared to those cultivated without Si. That response had a direct impact on the tolerance index (TI). According to Lux et al. (2004), the TI is classified as low when the values are below 35%; intermediate with values between 35% and 60%; and high when above 60%. In this work, the *A. tenella* plants exposed to 100 and 200  $\mu\text{M}$  of Cd alone showed the lowest tolerance index values (53.31% and 28.06%, respectively).

However, when the medium was supplemented with Si, the plants exposed to Cd were more tolerant ( $\geq 61.65\%$ ). Therefore, we can state that Si can mitigate the deleterious effects of Cd in *A. tenella* plants because these plants were more physiologically tolerant.

## Conclusion

Cadmium and silicon can modulate the physiological and anatomical responses of *A. tenella* plants. The presence of Si can mitigate the stress caused by Cd, as shown by the lesser presence of deleterious effects in the content of the photosynthetic pigments and the greater conservation of energy along the electron transport chain. Those responses permit a greater accumulation of biomass and higher tolerance to Cd.

## Abbreviations

ABS/RC – Absorption flux per reaction center (RC); Chl *a* – chlorophyll *a*; Chl *b* – chlorophyll *b*; Chl *total* – total chlorophyll;  $DI_0/RC$  – Dissipated energy flux per RC;  $F_0$  – Initial fluorescence;  $F_m$  – maximal fluorescence intensity;  $F_t$  – fluorescence at time *t* after start of actinic illumination;  $F_V/F_0$  – ratio of the de-excitation rate constants for photochemical and nonphotochemical events;  $PI_{(ABS)}$  – performance index based on absorption;  $PI_{(Total)}$  – total performance index, which measures the performance up until the final electron acceptors of PSI; RC/ABS – total number of active reaction center;  $V_L$  – relative variable fluorescence at 0.15 ms (step L);  $V_I$  – relative variable fluorescence at 30 ms (step I);  $V_J$  – relative variable fluorescence at 2 ms (step J);  $V_K$  – relative variable fluorescence at 0.3 ms (step K);  $W_K$  – represents the damage to oxygen-evolving complex;  $W_L$  – indicates disturbance in the thylakoid membranes, reducing the energetic connectivity between the PSII units;  $\phi P_0$  – maximum quantum yield of primary photochemistry (at  $t = 0$ );  $\phi E_0$  – quantum yield of electron transport (at  $t = 0$ );  $\phi D_0$  – quantum yield of energy dissipation (at  $t = 0$ );  $\delta R_0$  – Efficiency/probability with which an electron from the intersystem electron carriers moves to reduce end electron acceptors at the PSI acceptor side (RE).

## Declarations

## Author contributions:

FPR, SWM, EC, PCSB, and LTC performed experiments. FPR and JPRM wrote the manuscript and performed the statistical analysis. ARF and ABPLG provided the structure and contributed to the design and interpretation of the results. All the authors have read and approved the manuscript.

## Acknowledgments:

The authors acknowledge the scholarship granted by CAPES (Coordination for the Improvement of Higher Education Personnel), and FAPES (Espírito Santo Research Foundation). The authors also acknowledge

Luiz Carlos de Almeida Rodrigues for technical assistance in making the figures.

## References

1. Acosta-Motos JR, Diaz-Vivancos P, Alvarez S, Fernández-García N, Sanchez-Blanco MJ, Hernández JA (2015) NaCl-induced physiological and biochemical adaptive mechanisms in the ornamental *Myrtus communis* L. plants. *J Plant Physiol* 183:41–51. <https://doi.org/10.1016/j.jplph.2015.05.005>
2. Adrees M, Ali S, Rizwan M, Zia-Ur-Rehman M, Ibrahim M, Abbas F, Farid M, Qayyum MF, Irshad MK (2015) Mechanisms of silicon-mediated alleviation of heavy metal toxicity in plants: a review. *Ecotoxicol Environ Saf* 119:186–197. <https://doi.org/10.1016/j.ecoenv.2015.05.011>
3. Arnon DI (1949) Copper enzymes in isolated chloroplasts. Polyphenoloxidase in *Beta vulgaris*. *Plant Physiol* 24(1):1–15. <https://doi.org/10.1104/pp.24.1.1>
4. Bari MA, Prity SA, Das U, Akther MS, Sajib SA, Reza MA, Kabir AH (2020) Silicon induces phytochelatin and ROS scavengers facilitating cadmium detoxification in rice. *Plant Biol* 22(3):472–479. <https://doi.org/10.1111/plb.13090>
5. Begovic L, Galic V, Abicic I, Loncaric Z, Lalic A, Mlinaric S (2020) Implications of intra-seasonal climate variations on chlorophyll a fluorescence and biomass in winter barley breeding program. *Photosynthetica* 58(4):995–1008. <https://doi.org/10.32615/ps.2020.053>
6. Bhat JA, Shivaraj S, Singh P, Navadagi DB, Tripathi DK, Dash PK, Solanke AU, Sonah H, Deshmukh R (2019) Role of silicon in mitigation of heavy metal stresses in crop plants. *Plants* 8(3):71. <https://doi.org/10.3390/plants8030071>
7. Brestic M, Zivcak M, Kalaji HM, Carpentier R, Allakhverdiev SI (2012) Photosystem II thermostability in situ: environmentally induced acclimation and genotype-specific reactions in *Triticum aestivum* L. *Plant Physiol Biochem* 57:93–105. <https://doi.org/10.1016/j.plaphy.2012.05.012>
8. Cai Y, Zhang S, Cai K, Huang F, Pan B, Wang W (2020) Cd accumulation, biomass and yield of rice are varied with silicon application at different growth phases under high concentration cadmium-contaminated soil. *Chemosphere* 242:125–128. <https://doi.org/10.1016/j.chemosphere.2019.125128>
9. Chung YS, Kim SH, Park CW, Na CI, Kim Y (2020) Treatment with silicon fertilizer induces changes in root morphological traits in soybean (*Glycine max* L.) during early growth. *J Crop Sci Biotech* 23:445–451. <https://doi.org/10.1007/s12892-020-00052-7>
10. Corso D, Delzon S, Lamarque LJ, Cochard H, Torres-Ruiz JM, King A, Brodrribb T (2020) Neither xylem collapse, cavitation, or changing leaf conductance drive stomatal closure in wheat. *Plant Cell Environ* 43(4):854–865. <https://doi.org/10.1111/pce.13722>
11. Ding Y, Wang Y, Zheng X, Cheng W, Shi R, Feng R (2017) Effects of foliar dressing of selenite and silicate alone or combined with different soil ameliorants on the accumulation of As and Cd and antioxidant system in *Brassica campestris*. *Ecotoxicol Environ Saf* 142:207–215. <https://doi.org/10.1016/j.ecoenv.2017.04.001>

12. Dobrikova AG, Apostolova EL, Hanć A, Yotsova E, Borisova P, Sperdouli I, Adamakis IDS, Moustakas M (2021) Cadmium toxicity in *Salvia sclarea* L.: An integrative response of element uptake, oxidative stress markers, leaf structure and photosynthesis. *Ecotoxicol Environ Saf* 209:118–151. <https://doi.org/10.1016/j.ecoenv.2020.111851>
13. Emamverdian A, Ding Y, Xie Y, Sangari S (2018) Silicon mechanisms to ameliorate heavy metal stress in plants. *Biomed Res Int* 20:258–279. <https://doi.org/10.1155/2018/8492898>
14. Etesami H, Jeong BR (2018) Silicon (Si): Review and future prospects on the action mechanisms in alleviating biotic and abiotic stresses in plants. *Ecotoxicol Environ Saf* 147:881–896. <https://doi.org/10.1016/j.ecoenv.2017.09.063>
15. Franić M, Galić V, Mazur M, Šimić D (2017) Effects of excess cadmium in soil on JIP-test parameters, hydrogen peroxide content and antioxidant activity in two maize inbreds and their hybrid. *Photosynthetica* 55:1–10. <https://doi.org/10.1007/s11099-017-0710-7>
16. Ferreira E, Cavalcanti P, Nogueira D (2018) *ExpDes*. pt: Experimental Designs package. R package version 1.2. 0. Retrieved Sept 11: 20–48
17. Grajek H, Rydzyński D, Piotrowicz-Cieślak A, Herman A, Maciejczyk M, Wieczorek Z (2020) Cadmium ion-chlorophyll interaction—Examination of spectral properties and structure of the cadmium-chlorophyll complex and their relevance to photosynthesis inhibition. *Chemosphere* 261:127434. <https://doi.org/10.1016/j.chemosphere.2020.127434>
18. Gu HH, Qiu H, Tian T, Zhan SS, Chaney RL, Wang SZ, Tang YT, Morel JL, Qiu RL (2011) Mitigation effects of silicon rich amendments on heavy metal accumulation in rice (*Oryza sativa* L.) planted on multi-metal contaminated acidic soil. *Chemosphere* 83:1234–1240. <https://doi.org/10.1016/j.chemosphere.2011.03.014>
19. Guo Y, Zhang Y, Lu Y, Shi J, Chen S, Strasser R, Qiang S, Hu Z (2020) Effect of AtLFNR1 deficiency on chlorophyll *a* fluorescence rise kinetics OJIP of *Arabidopsis*. *Photosynthetica* 58(2):391–398. <https://doi.org/10.32615/ps.2019.167>
20. Haider FU, Liqun C, Coulter JA, Cheema SA, Wu J, Zhang R, Wenjun M, Farooq M (2021) Cadmium toxicity in plants: Impacts and remediation strategies. *Ecotoxicol Environ Saf* 211:111–127. <https://doi.org/10.1016/j.ecoenv.2020.111887>
21. Houry T, Khairallah Y, Al Zahab A, Osta B, Romanos D, Haddad G (2020) Heavy metals accumulation effects on the photosynthetic performance of geophytes in Mediterranean reserve. *J King Saud Univ Sci* 32(1):874–880. <https://doi.org/10.1016/j.jksus.2019.04.005>
22. Hu B, Shao S, Ni H, Fu Z, Hu L, Zhou Y, Min X, She S, Chen S, Huang M, Zhou L, Li Y, Shi Z (2020) Current status, spatial features, health risks, and potential driving factors of soil heavy metal pollution in China at province level. *Environ Pollut* 266:114961. <https://doi.org/10.1016/j.envpol.2020.114961>
23. Huang H, Li M, Rizwan M, Dai Z, Yuan Y, Hossain MM, Cao M, Xiong S, Tu S (2021) Synergistic effect of silicon and selenium on the alleviation of cadmium toxicity in rice plants. *J Hazard Mater* 401:123–149. <https://doi.org/10.1016/j.jhazmat.2020.123393>

24. Janečková H, Husičková A, Lazár D, Ferretti U, Pospíšil P, Špundová M (2019) Exogenous application of cytokinin during dark senescence eliminates the acceleration of photosystem II impairment caused by chlorophyll b deficiency in barley. *Plant Physiol Biochem* 136:43–51. <https://doi.org/10.1016/j.plaphy.2019.01.005>
25. Johansen DA (1940) *Plant microtechnique*. McGraw-Hill Book Company, Inc, pp 530–550
26. Kalaji HM, Jajoo A, Oukarroum A, Brestic M, Zivcak M, Samborska IA, Cetner MD, Łukasik I, Goltsev V, Ladle RJ (2016) Chlorophyll *a* fluorescence as a tool to monitor physiological status of plants under abiotic stress conditions. *Acta Physiol Plant* 4:1–11. <https://doi.org/10.1007/s11738-016-2113-y>
27. Klotzbücher A, Klotzbücher T, Jahn R, Van Chien H, Hinrichs M, Sann C, Vetterlein D (2018) Effects of Si fertilization on Si in soil solution, Si uptake by rice, and resistance of rice to biotic stresses in Southern Vietnam. *Paddy Water Environ* 16(2):243–252. <https://doi.org/10.1007/s10333-017-0610-2>
28. Liu L, Li W, Song W, Guo M (2018) Remediation techniques for heavy metal-contaminated soils: Principles and applicability. *Sci Total Environ* 633:206–219. <https://doi.org/10.1016/j.scitotenv.2018.03.161>
29. Lux A, Sottnikova A, Opatrna J, Greger M (2004) Differences in structure of adventitious roots in *Salix* clones with contrasting characteristics of cadmium accumulation and sensitivity. *Physiol Plant* 120(4):537–545. <https://doi.org/10.1111/j.0031-9317.2004.0275.x>
30. Malhotra C, Kapoor RT (2019) Silicon: a sustainable tool in abiotic stress tolerance in plants. In: Hasanuzzaman M, Hakeem KR, Nahar K, Alharby HF (eds) *Plant Abiotic Stress Tolerance*. Springer, Cham, Switzerland, pp 333–356. [https://doi.org/10.1007/978-3-030-06118-0\\_14](https://doi.org/10.1007/978-3-030-06118-0_14)
31. Martins JPR, Rodrigues LCA, Silva TS, Santos ER, Falqueto AR, Gontijo ABPL (2019) Sources and concentrations of silicon modulate the physiological and anatomical responses of *Aechmea blanchetiana* (Bromeliaceae) during in vitro culture. *Plant Cell Tissue Organ Cult* 137:397–410. <https://doi.org/10.1007/s11240-019-01579-6>
32. Martins JPR, Conde LT, Falqueto AR, Gontijo ABPL (2021) Selenium biofortified *Aechmea blanchetiana* (Bromeliaceae) can resist lead-induced toxicity during in vitro culture. *Acta Physiol Plant* 43:149. <https://doi.org/10.1007/s11738-021-03323-0>
33. Martins JPR, Souza AFC, Rodrigues LCA, Braga PCS, Gontijo ABPL, Falqueto AR (2020a) Zinc and selenium as modulating factors of the anatomy and physiology of *Billbergia zebrina* (Bromeliaceae) during in vitro culture. *Photosynthetica* 58:1068–1077. <https://doi.org/10.32615/ps.2020.058>
34. Martins JPR, Vasconcelos LL, BRAGA PCS, Rossini FP, Conde LT, Rodrigues LCA, Falqueto AR, Gontijo ABPL (2020b) Morphophysiological responses, bioaccumulation and tolerance of *Alternanthera tenella* Colla (Amaranthaceae) to excess copper under in vitro conditions. *Plant Cell Tissue Organ Cult* 143(2):303–318. <https://doi.org/10.1007/s11240-020-01917-z>
35. Menegale MC, Castro GSA, Mancuso M (2015) Silício: interação com o sistema solo-planta. *J Agron Sci* 4:435–454

36. Murashige T, Skoog F (1962) A revised medium for rapid growth and bio assays with tobacco tissue cultures. *Physiol Plant* 15(3):473–497. <https://doi.org/10.1111/j.1399-3054.1962.tb08052.x>
37. Mott KA, Peak D (2018) Effects of the mesophyll on stomatal responses in amphistomatous leaves. *Plant Cell Environ* 41(12):2835–2843. <https://doi.org/10.1111/pce.13411>
38. Paradiso R, Arena C, De Micco V, Giordano M, Aronne G, De Pascale S (2017) Changes in leaf anatomical traits enhanced photosynthetic activity of soybean grown in hydroponics with plant growth-promoting microorganisms. *Front Plant Sci* 8:674. <https://doi.org/10.3389/fpls.2017.00674>
39. Pereira AS, Cortez PA, Almeida AAF, Prasad MNV, França MGC, Cunha M, Jesus RM, Mangabeira PAO (2017) Morphology, ultrastructure, and element uptake in *Calophyllum brasiliense* Cambess. (Calophyllaceae J. Agardh) seedlings under cadmium exposure. *Environ Sci Pollut Res* 24(18):176–188. <https://doi.org/10.1007/s11356-017-9187-y>
40. Pereira TS, Pereira TS, Souza CLFC, Lima EJA, Batista BL, Lobato AKS (2018) Silicon deposition in roots minimizes the cadmium accumulation and oxidative stress in leaves of cowpea plants. *Physiol Mol Biol Plant* 24(1):99–114. <https://doi.org/10.1007/s12298-017-0494-z>
41. Pires-Lira MF, Castro EM, Lira JMS, Oliveira C, Pereira FJ, Pereira MP (2020) Potential of *Panicum aquaticum* Poir. (Poaceae) for the phytoremediation of aquatic environments contaminated by lead. *Ecotoxicol Environ Saf* 193:110–136. <https://doi.org/10.1016/j.ecoenv.2020.110336>
42. Ranjbarfordoei A, Samson R, Van Damme P (2006) Chlorophyll fluorescence performance of sweet almond [*Prunus dulcis* (Miller) D. Webb] in response to salinity stress induced by NaCl. *Photosynthetica* 44(4):513–522. <https://doi.org/10.1007/s11099-006-0064-z>
43. Rodrigues LCA, Martins JPR, Júnior OA, Guilherme LRG, Pasqual M, Castro EM (2017) Tolerance and potential for bioaccumulation of *Alternanthera tenella* Colla to cadmium under in vitro conditions. *Plant Cell Tissue Organ Cult* 130:507–519. <https://doi.org/10.1007/s11240-017-1241-4>
44. Roupael Y, De Micco V, Arena C (2017) Effect of *Ecklonia maxima* seaweed extract on yield, mineral composition, gas exchange, and leaf anatomy of zucchini squash grown under saline conditions. *J Appl Phycol* 29:459–470. <https://doi.org/10.1007/s10811-016-0937-x>
45. Roychowdhury A, Datta R, Sarkar D (2018) Heavy metal pollution and remediation. In: Török B, Dransfield T (eds) *Green Chemistry*. University of Massachusetts Boston, Boston, MA,, pp 359–373. United States, <https://doi.org/10.1016/B978-0-12-809270-5.00015-7>
46. Santos ER, Martins JPR, Rodrigues LCA, Gontijo ABPL, Falqueto AR (2020) Morphophysiological responses of *Billbergia zebrina* Lindl. (Bromeliaceae) in function of types and concentrations of carbohydrates during conventional in vitro culture. *Ornam Hort* 26:18–34. <https://doi.org/10.1590/2447-536X.v26i1.2092>
47. Scholz AK, Klepsch M, Karimi Z, Jansen S (2013) How to quantify conduits in wood? *Front Plant Sci* 4:56. <https://doi.org/10.3389/fpls.2013.00056>
48. Silva-Cunha LF, Oliveira VP, Nascimento AWS, Silva BRS, Batista BL, Alsahli AA, Lobato AKS (2021) Leaf application of 24-epibrassinolide mitigates cadmium toxicity in young *Eucalyptus urophylla*

- plants by modulating leaf anatomy and gas exchange. *Physiol Plant* 173:67–87.  
<https://doi.org/10.1111/ppl.13182>
49. Stirbet A, Govindjee SA (2011) On the relation between the Kautsky effect (chlorophyll a fluorescence induction) and Photosystem II: Basics and applications of the OJIP fluorescence transient. *J Photoch Photobio* 104:236–257. <https://doi.org/10.1016/j.jphotobiol.2010.12.010>
50. Strasser RJ, Tsimilli-Michael M, Srivastava A (2004) Analysis of the Chlorophyll *a* Fluorescence Transient. In: Papageorgiou GC, Govindjee (eds) *Chlorophyll a Fluorescence. Advances in Photosynthesis and Respiration*, vol 19. Springer, Dordrecht, pp 321–362.  
[https://doi.org/10.1007/978-1-4020-3218-9\\_12](https://doi.org/10.1007/978-1-4020-3218-9_12)
51. Suman J, Uhlik O, Viktorova J, Macek T (2018) Phytoextraction of heavy metals: a promising tool for clean-up of polluted environment? *Front Plant Sci* 9:1476. <https://doi.org/10.3389/fpls.2018.01476>
52. Ur-Rahman S, Xuebin Q, Zhao Z, Du Z, Imtiaz M, Mehmood F, Hongfei L, Hussain B, Ashraf MN (2021) Alleviatory effects of Silicon on the morphology, physiology, and antioxidative mechanisms of wheat (*Triticum aestivum* L.) roots under cadmium stress in acidic nutrient solutions. *Sci Rep* 11:1958. <https://doi.org/10.1038/s41598-020-80808-x>
53. Wellburn R (1994) The spectral determination of chlorophylls a and b, as well as total carotenoids, using various solvents with spectrophotometers of different resolution. *J Plant Physiol* 144(3):307–313. [https://doi.org/10.1016/S0176-1617\(11\)81192-2](https://doi.org/10.1016/S0176-1617(11)81192-2)
54. Wilkins DA (1957) A technique for the measurement of lead tolerance in plants. *Nature* 180:37–38. <https://doi.org/10.1038/180037b0>
55. Xiang M, Chen S, Wanga L, Donga Z, Huang J, Zhanga Y, Strasser RJ (2013) Effect of vulculic acid produced by *Nimbya alternantherae* on the photosynthetic apparatus of *Alternanthera hioxeroides*. *Plant Physiol Biochem* 65:81–88. <https://doi.org/10.1016/j.plaphy.2013.01.013>
56. Yanhui C, Hongrui W, Beining Z, Shixing G, Zihan W, Yue W, Huihui Z, Guangyu S (2020) Elevated air temperature damage to photosynthetic apparatus alleviated by enhanced cyclic electron flow around photosystem I in tobacco leaves. *Ecotoxicol Environ Saf* 204:111136. <https://doi.org/10.1016/j.ecoenv.2020.111136>
57. Vaculík M, Lukačová Z, Bokor B, Martinka M, Tripathi DK, Lux A (2020) Alleviation mechanisms of metal (loid) stress in plants by silicon: a review. *J Exp Bot* 71(21):6744–6757. <https://doi.org/10.1093/jxb/eraa288>
58. Zhang HH, Xu N, Wu X, Wang J, Ma S, Li X, Sun G (2018) Effects of four types of sodium salt stress on plant growth and photosynthetic apparatus in sorghum leaves. *J Plant Interact* 13(1):506–513. <https://doi.org/10.1080/17429145.2018.1526978>
59. Zhang L, Mcevoy D, Le Y, Ambrose C (2021) Live imaging of microtubule organization, cell expansion, and intercellular space formation in *Arabidopsis* leaf spongy mesophyll cells. *Plant Cell* 33:623–641. <https://doi.org/10.1093/plcell/koaa036>

## Tables

**Table 1** Characteristics of the anatomical structures of leaves of *A. tenella* plants cultivated with different cadmium (Cd) concentrations in the absence and presence of silicon (Si) during in vitro culture

Anatomical traits	0 $\mu\text{M}$ Si				40 $\mu\text{M}$ Si			
	0	50	100	200	0	50	100	200
	Cd ( $\mu\text{M}$ )				Cd ( $\mu\text{M}$ )			
Stomatal index (%)	18.8 $\pm$ 0.6 <sup>a</sup>	15.5 $\pm$ 0.8 <sup>ab</sup>	11.9 $\pm$ 0.9 <sup>b</sup>	8.2 $\pm$ 0.7 <sup>c</sup>	16.6 $\pm$ $\pm$ 1.0 <sup>A</sup>	15.8 $\pm$ 1.5 <sup>A</sup>	14.7 $\pm$ $\pm$ 0.9 <sup>A</sup>	13.2 $\pm$ 1.7 <sup>A*</sup>
Epidermal cell density (0.1 mm <sup>-2</sup> )	51.4 $\pm$ 0.3 <sup>b</sup>	54.4 $\pm$ 1.8 <sup>b</sup>	57.5 $\pm$ 3.9 <sup>b</sup>	83.4 $\pm$ 3.3 <sup>a*</sup>	57.7 $\pm$ $\pm$ 7.6 <sup>A</sup>	59.5 $\pm$ 1.9 <sup>A</sup>	63.6 $\pm$ $\pm$ 5.4 <sup>A</sup>	69.0 $\pm$ 6.3 <sup>A</sup>
Palisade parenchyma ( $\mu\text{m}$ )	80.1 $\pm$ 1.0 <sup>a*</sup>	55.9 $\pm$ 4.0 <sup>b</sup>	51.9 $\pm$ 2.4 <sup>b</sup>	58.2 $\pm$ 1.9 <sup>b*</sup>	67.8 $\pm$ $\pm$ 5.2 <sup>A</sup>	64.9 $\pm$ 2.1 <sup>A*</sup>	52.5 $\pm$ $\pm$ 1.7 <sup>B</sup>	53.1 $\pm$ 2.9 <sup>B</sup>
Spongy parenchyma ( $\mu\text{m}$ )	122 $\pm$ 6 <sup>a</sup>	85 $\pm$ 5 <sup>b</sup>	89 $\pm$ 5 <sup>b</sup>	116 $\pm$ 5 <sup>a</sup>	127 $\pm$ 5 <sup>A</sup>	107 $\pm$ $\pm$ 3 <sup>B*</sup>	80 $\pm$ 3 <sup>C</sup>	109 $\pm$ $\pm$ 5 <sup>AB</sup>

Means ( $\pm$  SE) followed by the same letter (lowercase for the absence of Si and uppercase for the presence of Si, comparing the concentrations of Cd) do not differ significantly between each other by the Tukey test at 5% probability. An asterisk (\*) denotes a significant difference between the absence and presence of Si at each Cd level according to the Tukey test at 5% probability.

**Table 2** Fresh and dry weight of the roots and aerial parts and tolerance index of *A. tenella* plants in the function of different concentrations of cadmium (Cd) in the absence and presence of silicon (Si) during in vitro culture

Growth traits	0 $\mu\text{M}$ de Si				40 $\mu\text{M}$ de Si			
	0	50	100	200	0	50	100	200
	Cd ( $\mu\text{M}$ )				Cd ( $\mu\text{M}$ )			
Fresh weight of roots (g plant <sup>-1</sup> )	0.30 $\pm$ 0.04 <sup>a</sup>	0.27 $\pm$ 0.03 <sup>a</sup>	0.26 $\pm$ 0.07 <sup>ab</sup>	0.11 $\pm$ 0.07 <sup>b</sup>	0.36 $\pm$ 0.04 <sup>A</sup>	0.26 $\pm$ 0.03 <sup>A</sup>	0.22 $\pm$ 0.02 <sup>A</sup>	0.16 $\pm$ 0.04 <sup>B*</sup>
Fresh weight of aerial part (g plant <sup>-1</sup> )	0.81 $\pm$ 0.11 <sup>a</sup>	0.69 $\pm$ 0.13 <sup>a*</sup>	0.34 $\pm$ 0.07 <sup>b</sup>	0.20 $\pm$ 0.04 <sup>b</sup>	0.70 $\pm$ 0.12 <sup>A</sup>	0.55 $\pm$ 0.04 <sup>B</sup>	0.43 $\pm$ 0.08 <sup>BC*</sup>	0.37 $\pm$ 0.04 <sup>C*</sup>
Dry weight of roots (g plant <sup>-1</sup> )	0.14 $\pm$ 0.02 <sup>a</sup>	0.12 $\pm$ 0.01 <sup>a</sup>	0.12 $\pm$ 0.3 <sup>a</sup>	0.05 $\pm$ 0.03 <sup>b</sup>	0.21 $\pm$ 0.02 <sup>A*</sup>	0.15 $\pm$ 0.01 <sup>B</sup>	0.13 $\pm$ 0.01 <sup>BC</sup>	0.10 $\pm$ 0.02 <sup>C*</sup>
Dry weight of aerial part (g plant <sup>-1</sup> )	0.37 $\pm$ 0.05 <sup>a</sup>	0.32 $\pm$ 0.06 <sup>a</sup>	0.15 $\pm$ 0.04 <sup>b</sup>	0.09 $\pm$ 0.02 <sup>b</sup>	0.41 $\pm$ 0.02 <sup>A</sup>	0.32 $\pm$ 0.07 <sup>B</sup>	0.25 $\pm$ 0.05 <sup>BC*</sup>	0.22 $\pm$ 0.02 <sup>C*</sup>
Tolerance index (%)	100.0 $\pm$ 16.0 <sup>a</sup>	86.5 $\pm$ 15.1 <sup>a</sup>	53.3 $\pm$ 20.0 <sup>b</sup>	28.1 $\pm$ 14.5 <sup>c</sup>	99.0 $\pm$ 17.5 <sup>A</sup>	92.0 $\pm$ 15.5 <sup>B</sup>	74.2 $\pm$ 9.1 <sup>C*</sup>	61.6 $\pm$ 16.2 <sup>D*</sup>

Means ( $\pm$  SE) followed by the same letter (lowercase for the absence of Si and uppercase for the presence of Si, comparing the concentrations of Cd) do not differ significantly between each other by the Tukey test at 5% probability. An asterisk (\*) denotes a significant difference between the absence and presence of Si at each Cd level according to the Tukey test at 5% probability.

## Figures

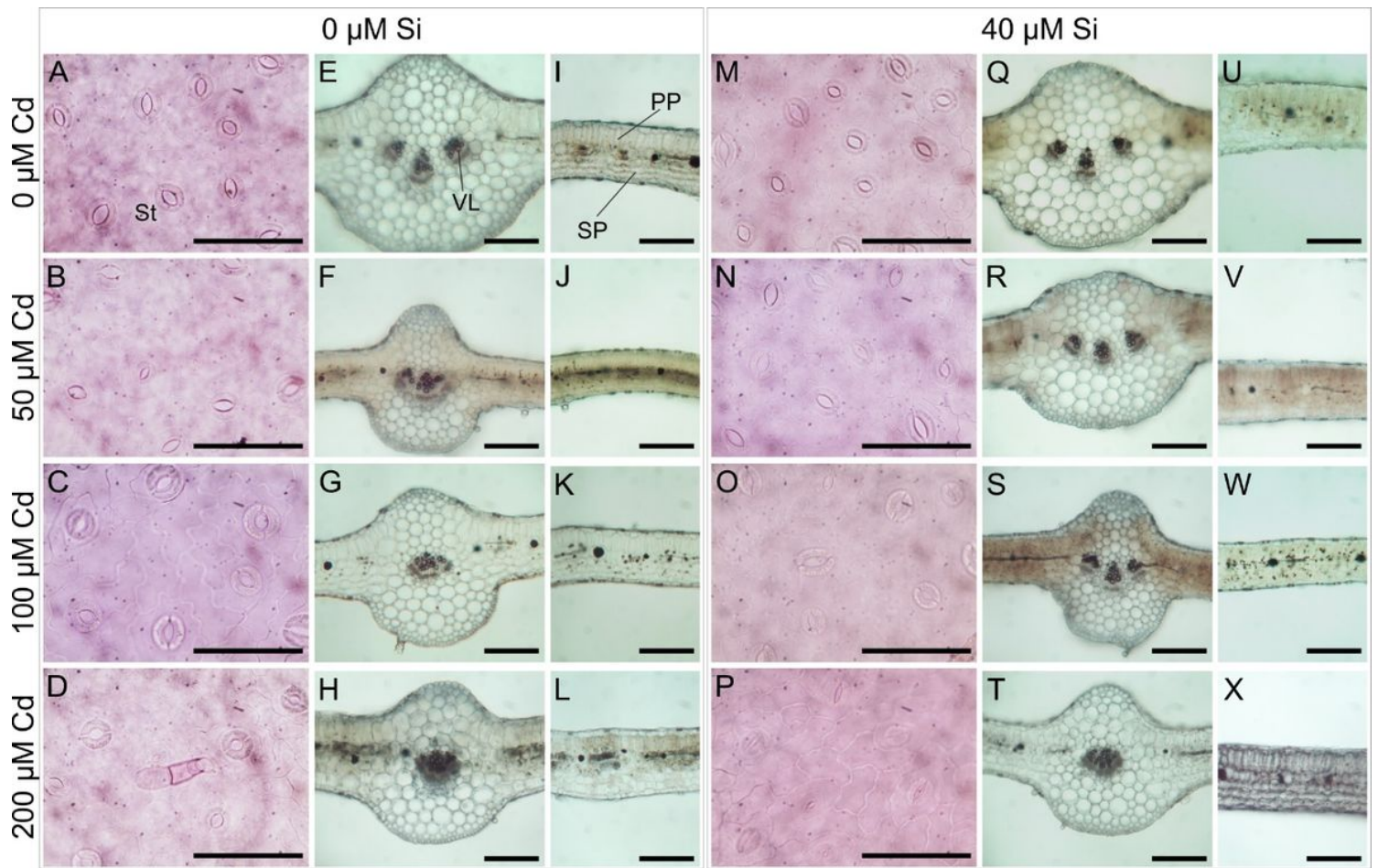


**Figure 1**

Paradermal sections (A – D and M – P) and transversal sections (E – L and Q – X) of leaves of *Alternanthera tenella* in the function of different concentrations of cadmium (Cd) in the absence and presence of silicon (Si) during in vitro culture. st - stomata, pp - palisade parenchyma, sp - spongy parenchyma, and vl - vessel elements. Bars = 100  $\mu$ m.

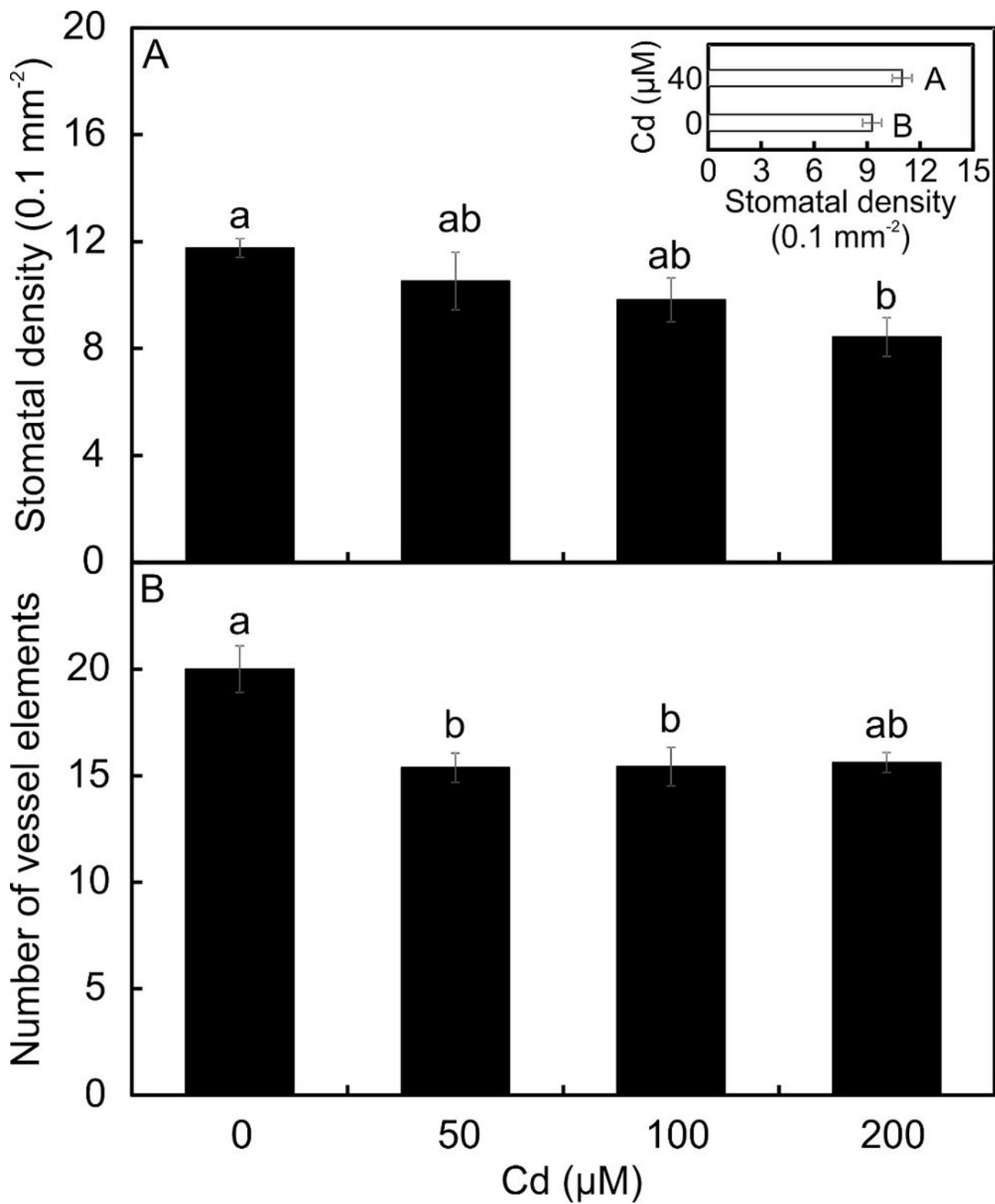


**Figure 2**

Stomatal density and number of vessel elements of *Alternanthera tenella* leaves in the function of different concentrations of cadmium (Cd) in the absence and presence of silicon (Si) during in vitro culture. Means ( $\pm$ SE) followed by the same letter do not differ significantly between each other by the Tukey test at 5% probability.

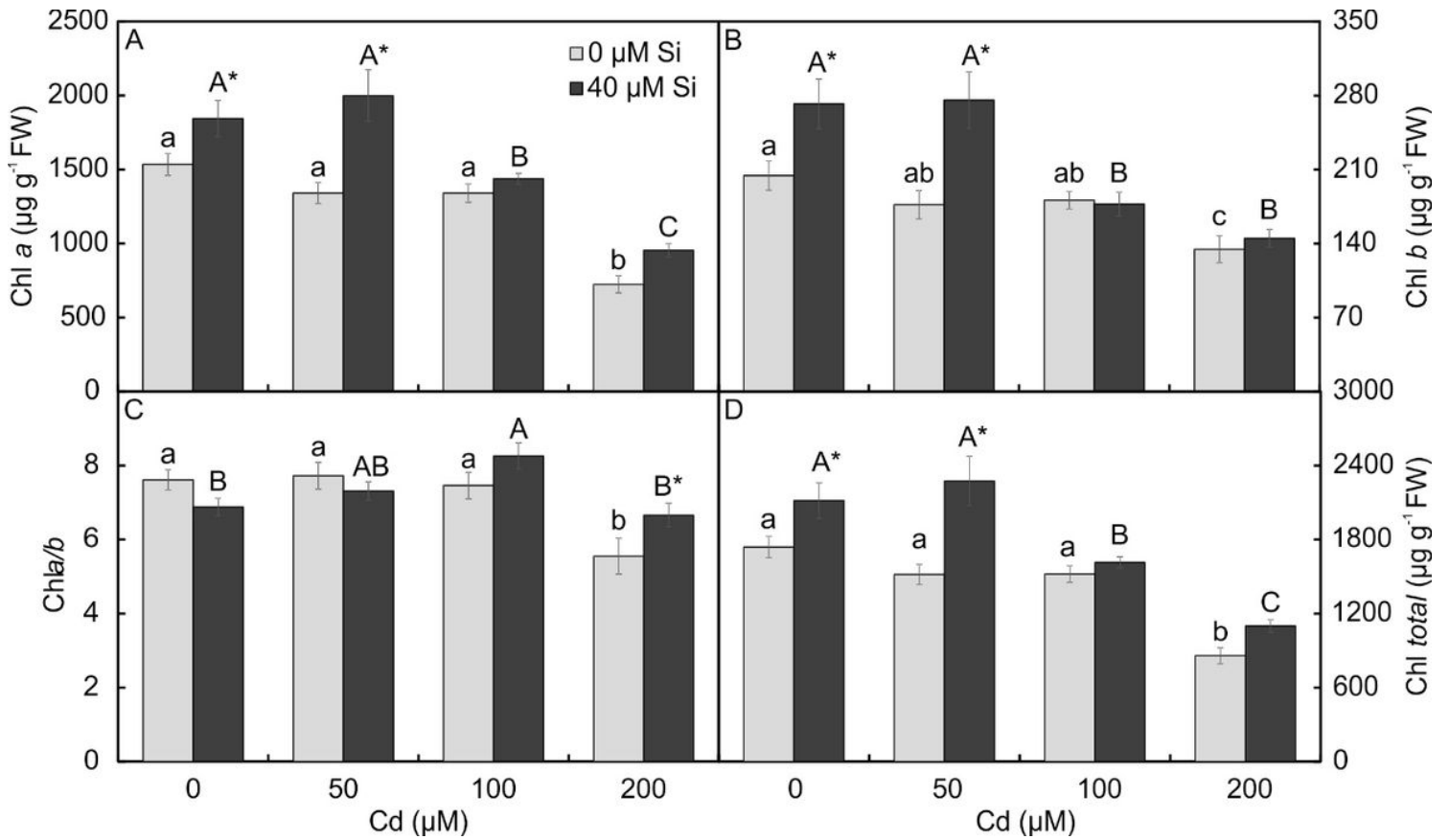


**Figure 3**

Content of photosynthetic pigments of *Alternanthera tenella* plants in the function of different concentrations of cadmium (Cd) in the absence and presence of silicon (Si) during in vitro culture. Means ( $\pm$  SE) followed by the same letter (lowercase for the absence of Si and uppercase for the presence of Si, comparing the concentrations of Cd) do not differ significantly between each other by the Tukey test at 5% probability. The asterisk (\*) denotes a significant difference between the absence and presence of Si at each Cd level according to the Tukey test at 5% probability.

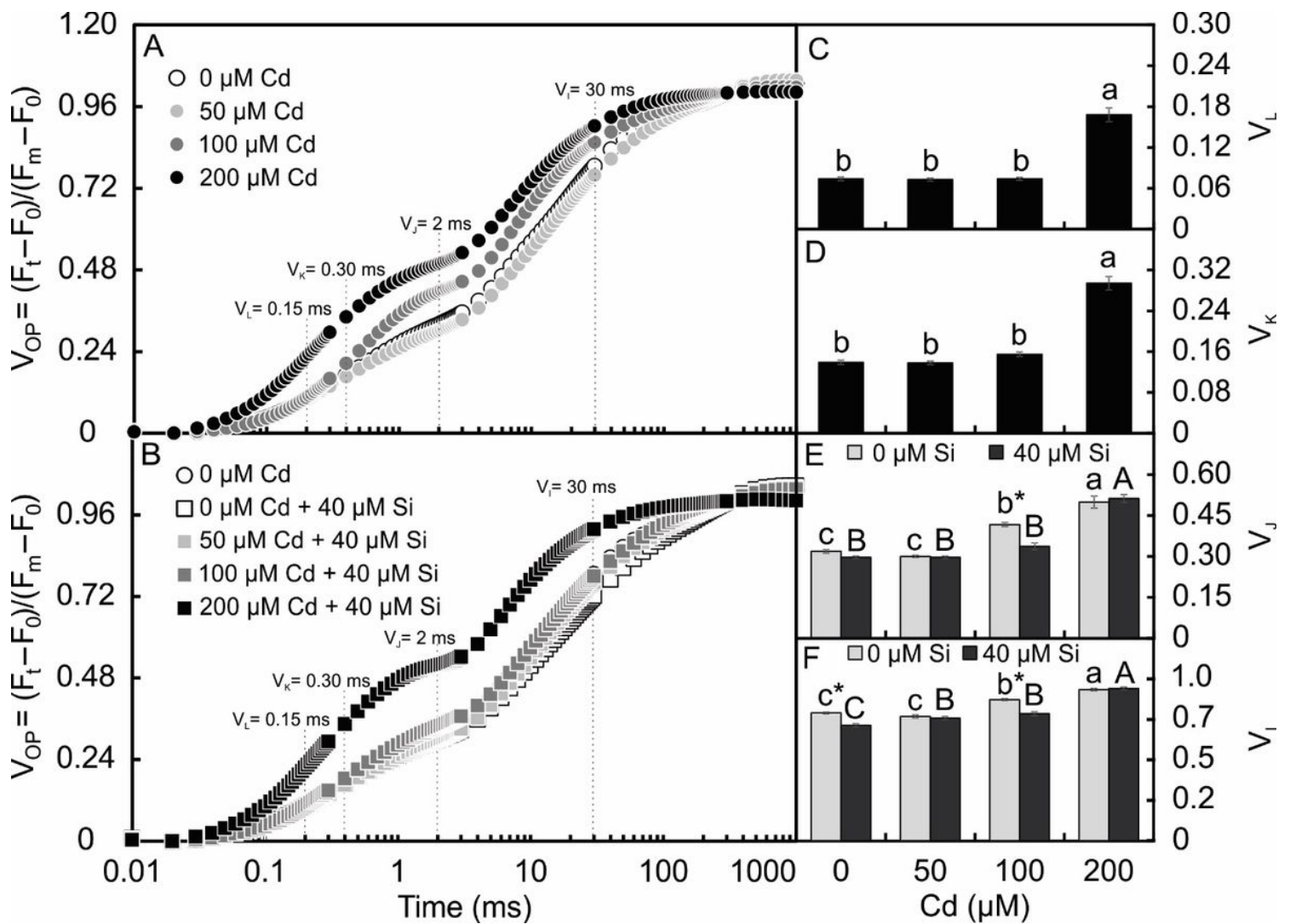


**Figure 4**

Relative variable fluorescence between steps O and P [ $V_{OP}$ ] (A); normalized variable fluorescence at step L [ $V_L$ ] (B), at step K [ $V_K$ ] (C), at step J [ $V_J$ ] (D), and at step I [ $V_I$ ] of *Alternanthera tenella* plants cultivated in vitro with different concentrations of cadmium (Cd) in the absence and presence of silicon. Means ( $\pm$  SE) followed by the same letter (lowercase for the absence of Si and uppercase for the presence of Si, comparing the concentrations of Cd) do not differ significantly between each other by the Tukey test at 5% probability. The asterisk (\*) denotes a significant difference between the absence and presence of Si at each Cd level according to the Tukey test at 5% probability.

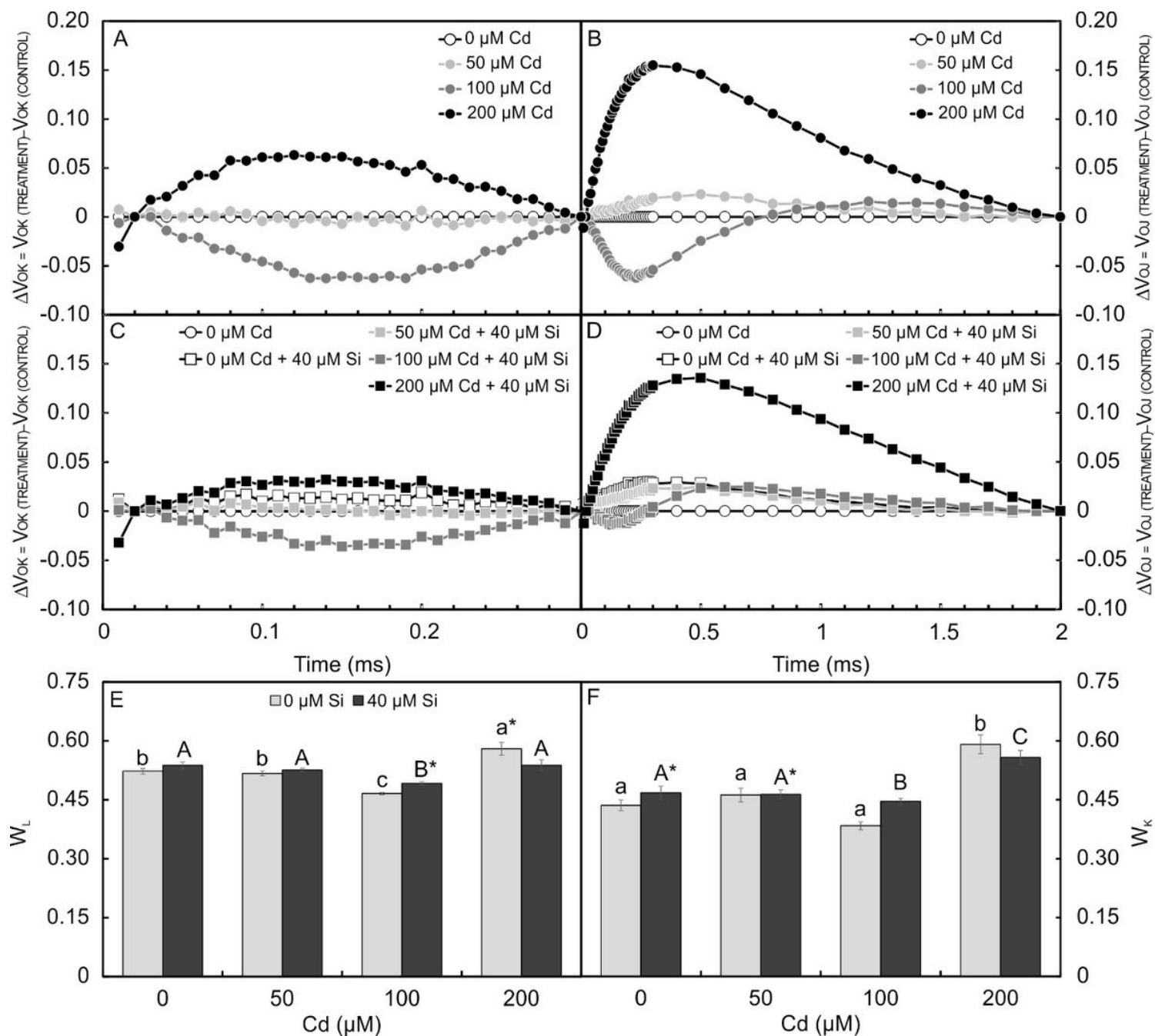


**Figure 5**

Kinetic differences between steps O and K [0.2 to 0.3 ms], steps O and J [0.2  $\mu\text{s}$  to 2 ms] in the absence of silicon (A) and presence of silicon (B); variable fluorescence between steps K and J [ $W_L$ ] (C) and between steps L and K [ $W_K$ ] (D) of *Alternanthera tenella* plants cultivated in vitro with different concentrations of cadmium (Cd) in the absence and presence of silicon. Means ( $\pm$  SE) followed by the same letter (lowercase for the absence of Si and uppercase for the presence of Si, comparing the concentrations of Cd) do not differ significantly between each other by the Tukey test at 5% probability. The asterisk (\*) denotes a significant difference between the absence and presence of Si at each Cd level according to the Tukey test at 5% probability.

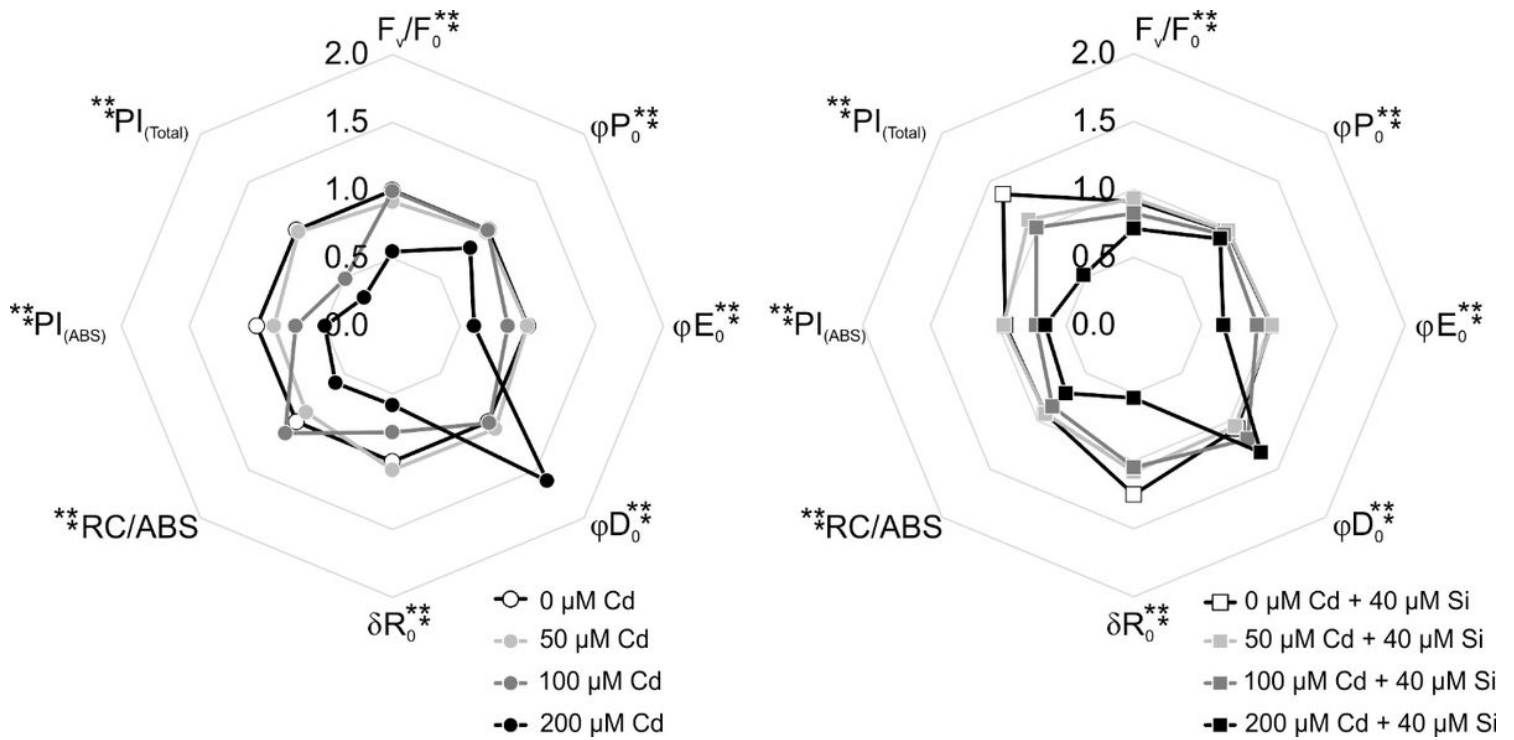


**Figure 6**

Parameters of the JIP test of *Alternanthera tenella* plants in the function of different concentrations of cadmium (Cd) in the absence and presence of silicon (Si) during in vitro culture. Means followed by an asterisk (\*) denote significant differences between the presence and absence of Si, while two asterisks (\*\*) denote significant differences between the concentrations of Cd at each level of Si according to the Tukey test at 5% probability. All the parameters of the JIP test are normalized in relation to the control (0 μM Si + 0 μM Cd = 1).

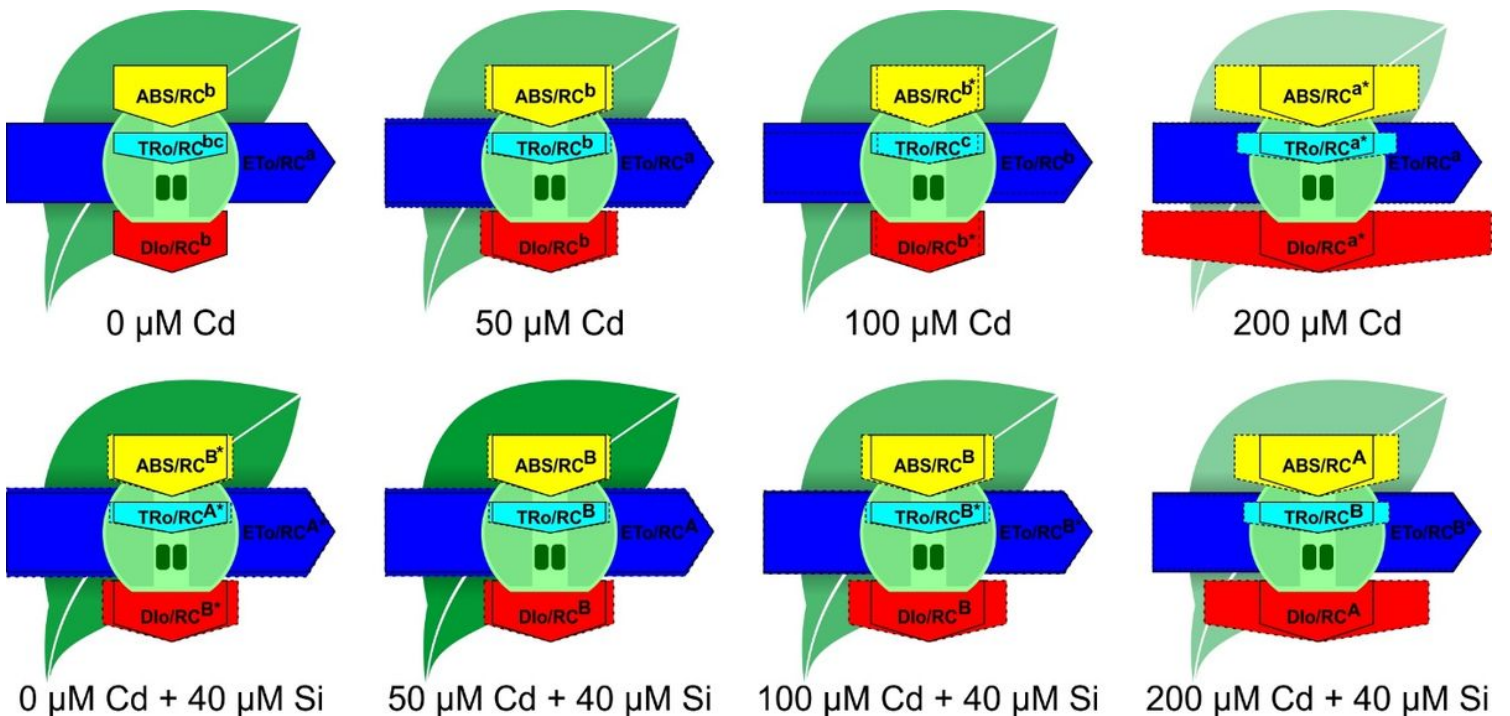


## Figure 7

Models of energy flux per reaction center (RC) in *Alternanthera tenella* leaves in the function of different concentrations of cadmium (Cd) in the absence and presence of silicon (Si) during in vitro culture. The level of green color of the leaf model indicates Chl *a* content (normalized from control treatment). Means ( $\pm$  SE) followed by the same letter (lowercase for the absence of Si and uppercase for the presence of Si, comparing the concentrations of Cd) do not differ significantly between each other by the Tukey test at 5% probability. An asterisk (\*) denotes a significant difference between the absence and presence of Si at each Cd level according to the Tukey test at 5% probability.